Spectrochimica Acta Part A: Molecular and Biomolecular Spectroscopy 226 (2020) 117625

Contents lists available at ScienceDirect

Spectrochimica Acta Part A: Molecular and Biomolecular Spectroscopy

journal homepage: www.elsevier.com/locate/saa

A merocyanine-based dual-mode optical probe for detection of hydrazine and its bioimaging application in vitro and vivo

Xiumei Guo [a], Shanshan Li [a], Shuai Mu [a], Yintang Zhang [b], Xiaoyan Liu [a,*], Haixia Zhang [a]

[a] State Key Laboratory of Applied Organic Chemistry, Key Laboratory of Nonferrous Metals Chemistry and Resources Utilization of Gansu Province and College of Chemistry and Chemical Engineering, Lanzhou University, Lanzhou, 730000, China
[b] Henan Key Laboratory of Biomolecular Recognition and Sensing, College of Chemistry and Chemical Engineering, Shangqiu Normal University, Shangqiu, 476000, China

ARTICLE INFO

Article history:
Received 26 February 2019
Received in revised form
20 July 2019
Accepted 6 October 2019
Available online 7 October 2019

Keywords:
Dual-mode detection
Hydrazine
Fluorescence probe
Bioimaging
In vivo

ABSTRACT

In this paper, a Merocyanine-based turn-on probe (**McyA**) has been developed for colorimetric and fluorescent dual-mode detection of N_2H_4 via an intra-molecular charge transfer (ICT) mechanism. In the presence of N_2H_4, the probe shows an obvious chromogenic response and fluorescent enhancement. Based on this feature, the synthesized **McyA** can be applied to quantify N_2H_4 concentration from 0.12 to 5.0 μM and 0.5−10 μM with a detection limit of 0.042 μM (1.3 ppb, S/N = 3) and 0.140 μM (4.5 ppb, S/N = 3), respectively. Moreover, **McyA** has also be successfully employed for imaging analysis of N_2H_4 distribution in different organs from the N_2H_4 ingested mice model, revealing the potential application of **McyA** as a powerful fluorescent sensor for tracking detection and risk assessment of hydrazine *in vivo*.

1. Introduction

Hydrazine (N_2H_4) is an essential reactive reactant in the preparation of polymers, pesticides, pharmaceuticals intermediated [1], emulsifiers and textile dyestuff [2−4]. Its strong reducing property enables its use as an oxygen scavenger and corrosion inhibitor in various applications including electric utilities [5], new materials, as well as an energetic fuel in missile and rocket propulsion system [6,7]. Besides, it is also used as an indispensable precursor in synthesis of hydrazine fuel cells in power generation sector [8]. However, N_2H_4 is extremely toxic and can be readily absorbed by biological systems during manufacture, usage, transportation and disposal [9,10], which cause carcinogenic and mutagenic effect [11]. Even worse, N_2H_4 has a volatile and high water solubility, which caused its ubiquitous distribution in the environment as well as in turn enters a route into human body through respiratory, dermal contact or food chain transfer. Thus, even for persons who are not chemists or industrial workers, the potential risk of them exposure to N_2H_4 is still existed. For these reasons, the U.S Environmental Protection Agency (EPA) has been implicated as a probable carcinogen with an allowable threshold limit value of 10 ppb [12,13]. Therefore, designing a facile and visualized detector for on-site and real-time recognition of N_2H_4 in a variety of matrices is very desirable.

To date, several different analytical methods for determination of N_2H_4 have been developed, including chromatography [14−17], electrochemistry [18], titrimetry [19], fluorometry [20−22] and so on. Among these analytical approaches, fluorescent techniques based on fluorescent probes [23−27] have received tremendous attention due to their high sensitivity, specificity, economy, simplicity for implementation, noninvasive and real-time detection in live cells or tissues. So far, numerous fluorescent probes for N_2H_4 detection have been explored based on the strong nucleophilicity of hydrazine toward the recognition moiety such as acetyl [28−32], formyl phenol [33], bromo butylate [34−36], levulinate [37−39], benzothiazole acetonitrile [40] and 2,4-dinitrophenyl [41]. Such probes are typically composed of an analyte-triggered site and a fluorophore. Undoubtedly, some of them show good selectivity and high sensitivity for detection of N_2H_4. However, from an economic, convenient and practical perspective, extra strategy such as construction of “naked-eye” and fluorescent dual-mode sensors for detection and bioimaging of N_2H_4 in vitro and vivo are still imperative.

Merocyanines are donor-acceptor-substituted conjugated systems (D-π-A) and shows a strong intramolecular charge transfer (ICT) character [42], which endow merocyanine unit potential

* Corresponding author.
E-mail address: liuxiaoy@lzu.edu.cn (X. Liu).

https://doi.org/10.1016/j.saa.2019.117625
1386-1425/

applications in optoelectronics [43], and as fluorescent sensors for biology imaging or medicine detection [44]. Driven by above requirement, we designed and synthesized a simple ratiometric colorimetric and fluorescent dual-mode probe (**McyA**) based on Merocyanine as fluorophore and acetyl group as recognition site for specific detection of N_2H_4. As depicted in Scheme 1, in the present of N_2H_4, N_2H_4 will attack the carbonyl group of the acetyl group and then lead to cleavage of the ester group, which produce the optical structure accompanying by changes in color and spectral properties under the physiological conditions [36]. Furthermore, the sensing mechanism of **McyA** for N_2H_4 was demonstrated by density functional theory (DFT) and high performance liquid chromatography (HPLC). Finally, **McyA** was employed for bioimaging of intracellular N_2H_4 and investigation of its bioaccumulation in animals.

2. Experimental section

2.1. Chemical reagents and instruments

2.1.1. Chemical reagents

1,2,3,3-Tetramethyl-3H-indole ($C_{12}H_{16}IN$,99%), p-hydroxybenzaldehyde ($C_7H_6O_2$,99%), bromo acetyl (C_2H_3BrO, 98%) were purchased from Anagji Chemicals (Shanghai, China). N_2H_4 was purchased from Saan Chemical Technology Co., Ltd. (Shanghai, China). Ultrapure water is purified by the ALH-6000-U instrument (America). other drugs and reagents were of analytical grade without further purification.

The stock 1.0 mM solution of **McyA** was prepared in DMSO. The following solutions (10.0 mM) were prepared in ultrapure water: N_2H_4, Cys, GSH, Glu, NH_2OH, urea, Aniline, thiourea, K^+, Ca^{2+}, Na^+, Mg^{2+}, Cu^{2+}, Zn^{2+}, Al^{3+}, Fe^{3+}, Hg^+, F^-, Br^-, Cl^-, I^-, ClO_4^-, ACO^-, CO_3^{2-}, $H_2PO_4^-$. The final concentration of **McyA** was 20 μM in phosphate buffer saline (PBS) buffer (10 mM, pH = 7.4, 20% DMSO).

2.1.2. Instruments

NMR spectra were measured using a JEOL400 MHz instruments (Japan). Mass spectra were analyzed using Brukermicr OTOF II with ESI mode (America). Absorption spectra were determined on a UV−visible spectrophotometer (TU-1810, China). Fluorescence spectra were recorded on a Fluorescence Spectrometer (RF-5301pc, Japan) with a Xenon lamp. The pH values were measured using a digital pH-meter (PHSJ-3F, Leici, Shanghai, China). Cell imaging was performed by Confocal fluorescence microscopy (FV1000, Olympus, Japan) and bioimaging was carried out with IVIS Spectrum (Canada) equipped with molecular imaging software 5.0.6.20. Chromatographic analysis was performed by Thermo Fisher's Dionex UltiMate 3000 HPLC (UHPLC, Chromatographic conditions: A = acetonitrile, B = ammonium acetate buffer solution, A = 90%, B = 10%; flow rate of 0.8 mL min^{-1}, detection wavelength: 445 nm)

2.2. Synthesis of probe(McyA)

The synthetic routes of probe **McyA** are shown in Fig. 1 and the details of procedure are described as follows.

2.2.1. Synthesis of McyOH

1,2,3,3-tetramethyl-3H-indoleiodide (903.5 mg, 3.0 mmol) and p-hydroxybenzaldehyde (439.6 mg, 3.6 mmol, 1.2 equiv) were mixed in 100 mL round-bottomed flask containing 40 mL of anhydrous ethanol. The mixture was heated to reflux for 12 h and monitored by thin layer chromatography (TLC). After the reaction was completed, the mixed solution was filtered and the filter cake was washed with petroleum ether to remove residual p-hydroxybenzaldehyde. Then, the crude product was dried at 60 °C. Subsequently, the product was purified and obtained the compound **McyOH** (yield 76%). ^{1}H NMR (400 MHz, DMSO-d_6) δ = 10.68 (s, 1H), 8.35 (d, *J* = 16.1 Hz, 1H), 8.10 (d, *J* = 8.7Hz,2H), 7.83 (d, *J* = 7.1 Hz, 2H), 7.60 (dt, *J* = 7.2, 5.8 Hz, 2H), 7.45 (d, *J* = 16.2 Hz, 1H), 6.97 (d, *J* = 8.6 Hz, 2H), 4.09 (s,3H), 1.78 (s, 6H).^{13}C NMR (101 MHz, DMSO-d_6) δ = 181.38, 163.19, 153.72, 143.17, 141.84, 133.56, 128.78, 125.98, 122.76, 116.40, 114.64, 109.30, 51.71, 34.05, 25.65.MS (ESI, *m*/*z*) Calcd.for [$C_{19}H_{20}INO$-I^-] = 278.3745, found: *m*/*z*278.3768.

2.2.2. Synthesis of probe McyA

Compound **McyOH** (80.8 mg, 0.2 mmol) was dissolved in 20 mL CH_2Cl_2, then triethylamine (Et_3N, 45 μL, 0.32 mmol, 2.0 equiv) was added. The mixture was stirred at 0 °C, and acetyl bromide (C_2H_3BrO, 30 μL, 0.4 mmol, 2.0 equiv) was added. After the reaction was finished (about 10 min), solvents were evaporated under reduced pressure and the solute was purified on a silica gel column (CH_2Cl_2/CH_3OH = 90:1) to give the desired product (yield 78%). ^{1}H NMR (400 MHz, DMSO-d_6) δ = 8.21 (dd, J = 12.4, 8.4 Hz, 3H), 7.76

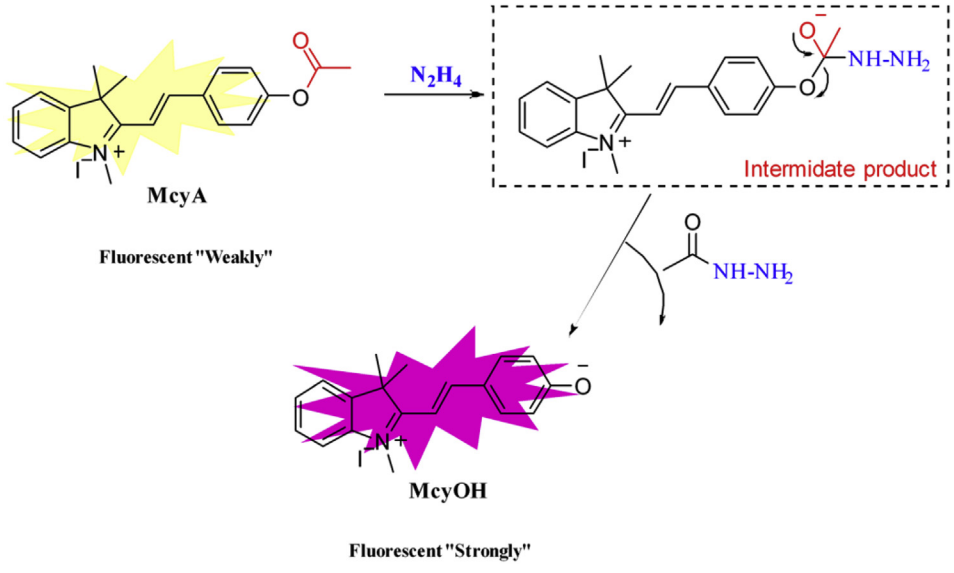

Scheme 1. Proposed Reaction of the Probe with N_2H_4.

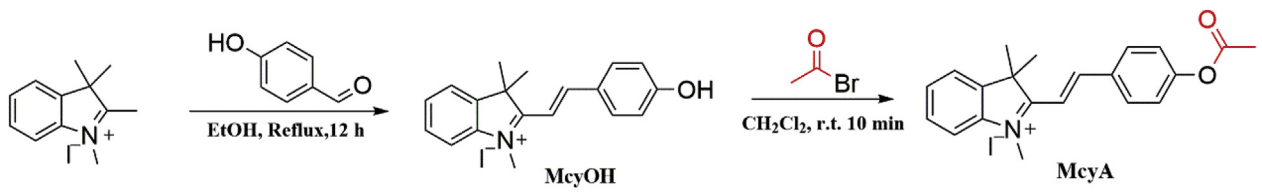

Fig. 1. Synthesis of fluorescent probe **McyA**.

(d, J = 16.2 Hz, 1H), 7.67 (dd, J = 5.9, 3.0 Hz, 1H), 7.62 − 7.56 (m, 3H), 7.29 (d, J = 8.7 Hz, 2H), 4.46 (s, 3H), 2.33 (s, 3H), 1.87 (s, 6H). ^{13}C NMR (101 MHz, DMSO-d_6) δ = 181.87, 168.84, 154.03, 151.76, 143.61, 141.79, 132.11, 131.86, 129.47, 128.95, 122.81, 115.31, 113.29, 52.26, 45.67, 34.72, 25.64, 25.18, 20.94. HRMS (ESI, *m/z*) Calcd. for [$C_{21}H_{22}INO_2$-I^-] = 320.4115 m/z, found: 320.2164 *m/z*.

2.3. General procedure for spectral measurement

A typical test solution was prepared by mixing 20 μL of **McyA** (1.0 mM) and 180 μL of DMSO, appropriate aliquot of each analyte stock solution and then supplementing to 1.0 mL with PBS buffer (10 mM, pH = 7.4). The resulting solution was shaken well at 37 °C for 20 min before the fluorescence and ultraviolet−visible (UV/Vis) absorption spectra were recorded. The fluorescence excitation and emission wavelength were 520 and 553 nm, respectively. The absorbance ($\lambda_{530}/\lambda_{385}$) was measured in an UV/Vis spectrograph.

2.4. Cytotoxicity assay

The cytotoxicity assay was manipulated with 3-(4,5-dimethyl-2-thiazolyl)-2,5-diphyl-2H-tetrazolium bromide (MTT) [45]. HepG2 cells (1×10^4 cells/pore plate) were seeded in a 96-well plate with 180 μL of cell suspension and incubated in 5% CO_2 at 37 °C for 24 h. The cells were treated with various concentration of **McyA** (0.0, 5.0, 10.0, 15.0, 20.0, 25.0, 50.0, 75.0, 100.0 μM) for 24 h, respectively. After washing twice with PBS buffer, MTT solution (5.0 mg mL^{-1}, PBS) was added into each well (10 μL/well, 0.5 mgmL^{-1}) and the residual MTT solution was removed by PBS solution after 4 h. Subsequently, 100 μM of DMSO was added into each well to dissolve the formazan crystals. After shaking for 10 min, the absorbance values of the wells were recorded using a microplate reader. The cytotoxic effect (VR) of probe **McyA** was assessed using the following equation: VR = A/A_0×100%. The assays were performed six replicates. The statistic mean values and standard derivation were utilized to estimate the cell viability.

2.5. In vivo imaging

2.5.1. Cell culture and imaging

HepG2 cells, grown in DMEM supplemented with heat-inactivated 10% (v/v) fetal bovine serum, 100 U mL^{-1} penicillin and 100 μg mL^{-1} streptomycin at 37 °C in 95% humidity and 5% CO_2 environment, were incubated with different concentrations of N_2H_4 (0.0, 3.0, 5.0, 50.0, 150.0 μM) at 37 °C for 20 min. Then, the cells were washed with PBS buffer to remove excrescent N_2H_4. Furthermore, the cells were treated by **McyA** (10 μM) for another 20 min. Finally, the cells were rinsed with PBS to remove the excessive **McyA** and the imaging of the cells was observed under Confocal microscopy at different times. The **McyA** emission was collected at 535−590 nm.

2.5.2. Mice skin-poptest

All animal experiments were performed in accordance with the guidelines issued by The Ethical Committee of Gansu College of Traditional Chinese Medicine. Kunming mice (KM, 7−8 weeks old) were given a skin-pop injection of **McyA**(100 μL, 50 μM in a mixture of PBS buffer (pH = 7.4, 10 mM, 20% DMSO), and given a subsequent skin-pop injection of N2H4 (50 μL, 500 μM in a mixture of PBS buffer (pH 7.4, 10 mM, 20% DMSO). The fur was removed by using 8% Na_2S aqueous solution and the mice were placed under general anesthetic through intraperitoneal injection with 10% chloral hydrate before imaging.

2.5.3. Bioaccumulation tests of N_2H_4 in mice

For tissues imaging, the mice were divided into four groups. The first group of mice was the control group, which were feed with normal drinking water for two days. The other three groups of the mice were feed with drink water containing the different concentration (5, 10, 15 ppb) of N_2H_4 for two days. Then, these mice were euthanized and the organs were dissected and directly soaked in 50 μM **McyA** in PBS buffer (10 mM, pH = 7.4, 20% DMSO) solution for 20 min. Subsequently, these treated organs (heart, liver, lung,

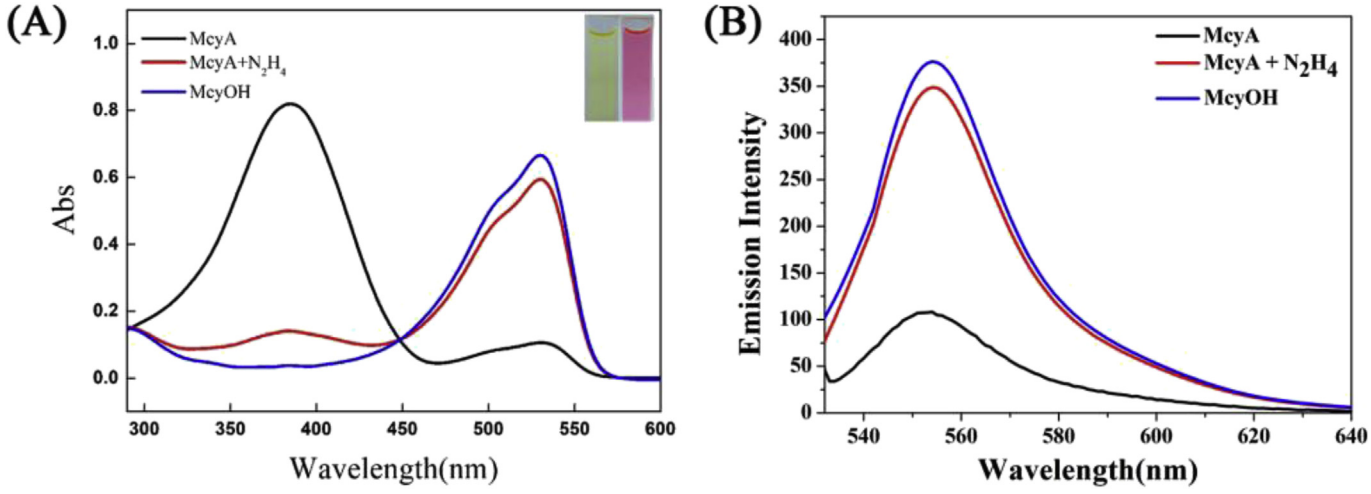

Fig. 2. (A) UV/Vis absorption (A) and fluorescence emission spectra (B) of the **McyOH** and **McyA** probe (20 μM) before (black line) and after reacted with N_2H_4 (200 μM) (red line), and **McyOH** (blue line). The detection system was DMSO/H_2O solution (1:4, v/v, 10 mM PBS, pH = 7.4, Ex = 520 nm).

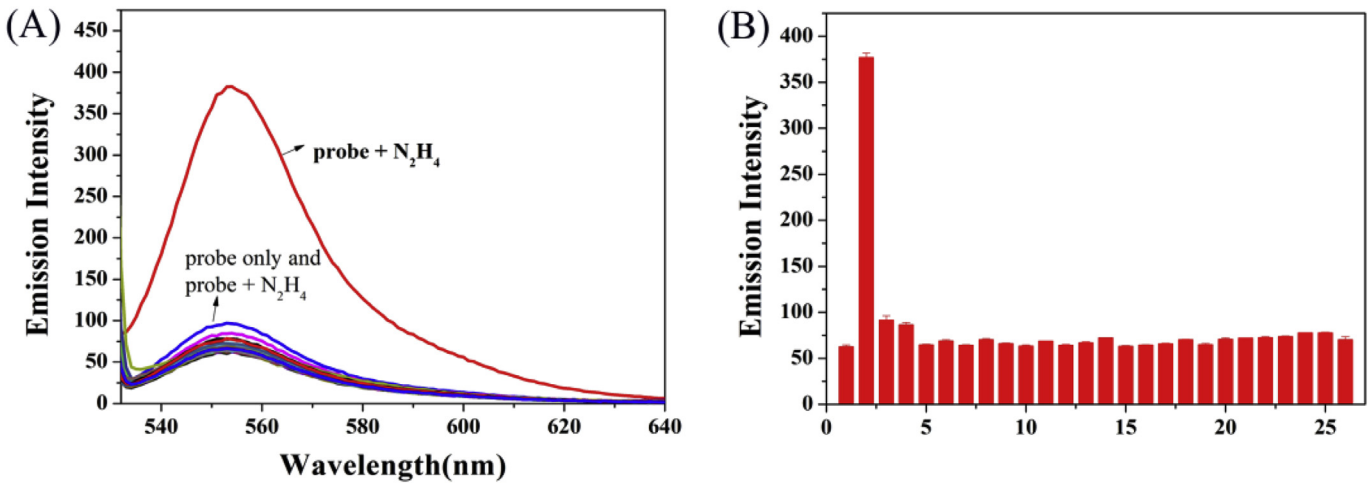

Fig. 3. (A) Fluorescence spectra of probes (20 μM) in response to N_2H_4 and other analytes (150 μM). 1. Blank probe, 2. N_2H_4, 3. Cys, 4. GSH, 5. Gln, 6. Hydroxylamine, 7. Urea, 8. Aniline, 9. Thiourea, 10. K^+, 11. Ca^{2+}, 12. Na^+, 13. Mg^{2+}, 14. Cu^{2+}, 15. Zn^{2+},16. Al^{3+}, 17. Fe^{3+}, 18. Hg^+, 19. F^-, 20. Br^-, 21. Cl^-, 22. I^-, 13. ClO_4^-, 24. Ac^-, 25. CO_3^{2-}, 26. $H_2PO_4^-$. Fluorescence changes were recorded after incubation at 37 °C for 20 min. The error bars had three groups of standard deviations with parallel data.

kidney, spleen and stomach) were observed under Confocal microscopy and the emission was collected at 535−590 nm.

3. Results and discussion

3.1. Synthesis of probe McyA

Based on the concept of simple and fast, the probe (**McyA**) was synthesized by one-step reaction of McyOH with acetyl bromide as described in Fig. 1. The structures of McyOH and McyA were demonstrated by analysis of ^{1}H NMR, ^{13}C NMR, and ESI-MS data (Figs. S1, S2, S3, S4 and S5 in the Electronic Supplementary Information).

3.2. UV−vis absorption and fluorescence spectra

In order to verify the feasibility of detecting the N_2H_4 by the probe, we first evaluated spectral properties of **McyA** in the presence and absence of N_2H_4 in PBS buffer (10 mM, pH = 7.4, 20% DMSO), respectively. As shown in Fig. 2A, the **McyA** itself exhibits a strong absorption band at 385 nm. However, upon reaction with N_2H_4 for 20 min, the absorption band at 385 nm almost disappears and subsequently a new band at 530 nm appears evidently, which corresponds to the UV characteristic peak of **McyOH.** Simultaneously, the color of the **probe** changed from faint yellow to pink under natural light (Inset of Fig. 2A), allowing ratiometric colorimetric detection of N_2H_4 by the naked eye. Accordingly, an obvious enhancement fluorescent signal can be observed at 553 nm upon excitation at 520 nm (Fig. 2B). These results are in line with our design concept.

3.3. Selectivity of McyA to N_2H_4

To verify the selectivity, the fluorescence responses of **McyA** toward different analytes were performed in PBS buffer solution (10 mM, pH 7.4, 20% DMSO). As shown in Fig. 3A and B, Addition of

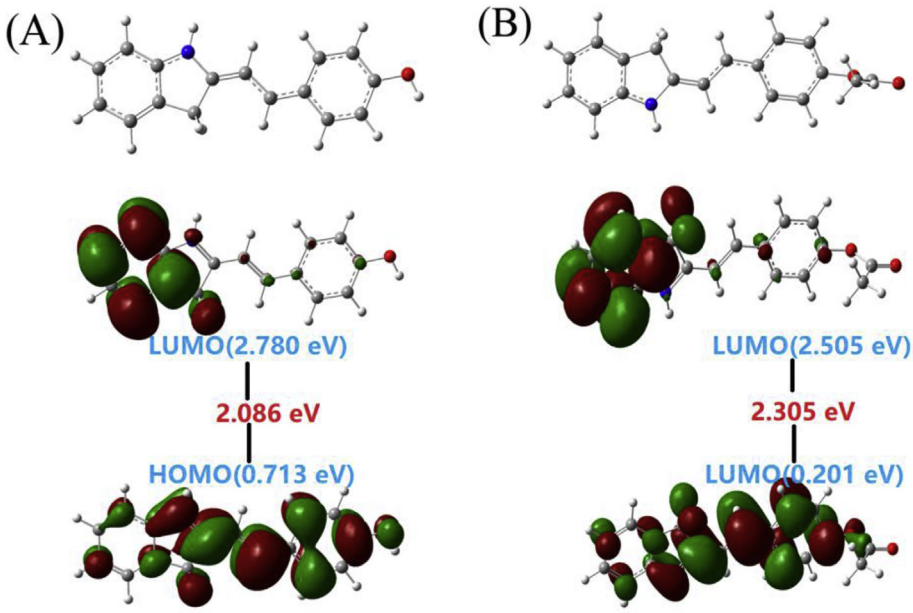

Fig. 4. McyOH (A) and McyA (B) optimize structure and frontier orbital calculations through density functional theory (DFT) (B3LYP/6-311G (d, p)/level, Gaussian 09). In the stick model, carbon, oxygen, and nitrogen atoms are labeled as gray, red, and blue, respectively.

N_2H_4 to the **McyA** solution leads to a strong fluorescence enhancement at 553 nm. However, various analytes (150 μM, Cys, GSH, Gln, hydroxylamine, urea, aniline, thiourea, K^+, Ca^{2+}, Na^+, Mg^{2+}, Cu^{2+}, Zn^{2+}, Al^{3+}, Fe^{3+}, Hg^+, F^-, Br^-, Cl^-, I^-, ClO_4^-, Ac^-, CO_3^{2-}, $H_2PO_4^-$) exhibit almost no interaction with the probe. Additionally, the competitive experiments demonstrate that the specificity of the probe **McyA** for N_2H_4 is prominent over other interfering analytes under physiological conditions (Figs. S6A and S6B).

3.4. The proposed mechanism of probe in sensing N_2H_4

In theory, the merocyanine chromophores have conjugated π-electrons and a push-pull structural element. **McyOH** molecule is composed of a phenol latent donor (push) in conjugation with one acceptor (2,3-dihydro-1H-xanthene-indolium, pull). Upon formation of a phenolate ion, the latent donor is turn on, which enables an ICT from the activated donor to the acceptor to form a new push-pull conjugated system. Thus, the push-pull system of **McyOH** molecule can emit strong fluorescence. However, since the electron-withdrawing acetyl group in **McyA** hinders the progress of ICT, it weakens the fluorescence of the original fluorophore. In order to verify this speculation, we performed a computational study using a suit of Gaussian 09 programs [density functional theory (DFT) at the B3LYP/6-311G (d, p)level] [46–48]. The structures of **McyA** and **McyOH** were optimized and their frontier molecular orbital energies were calculated (Fig. 4). The results show that the

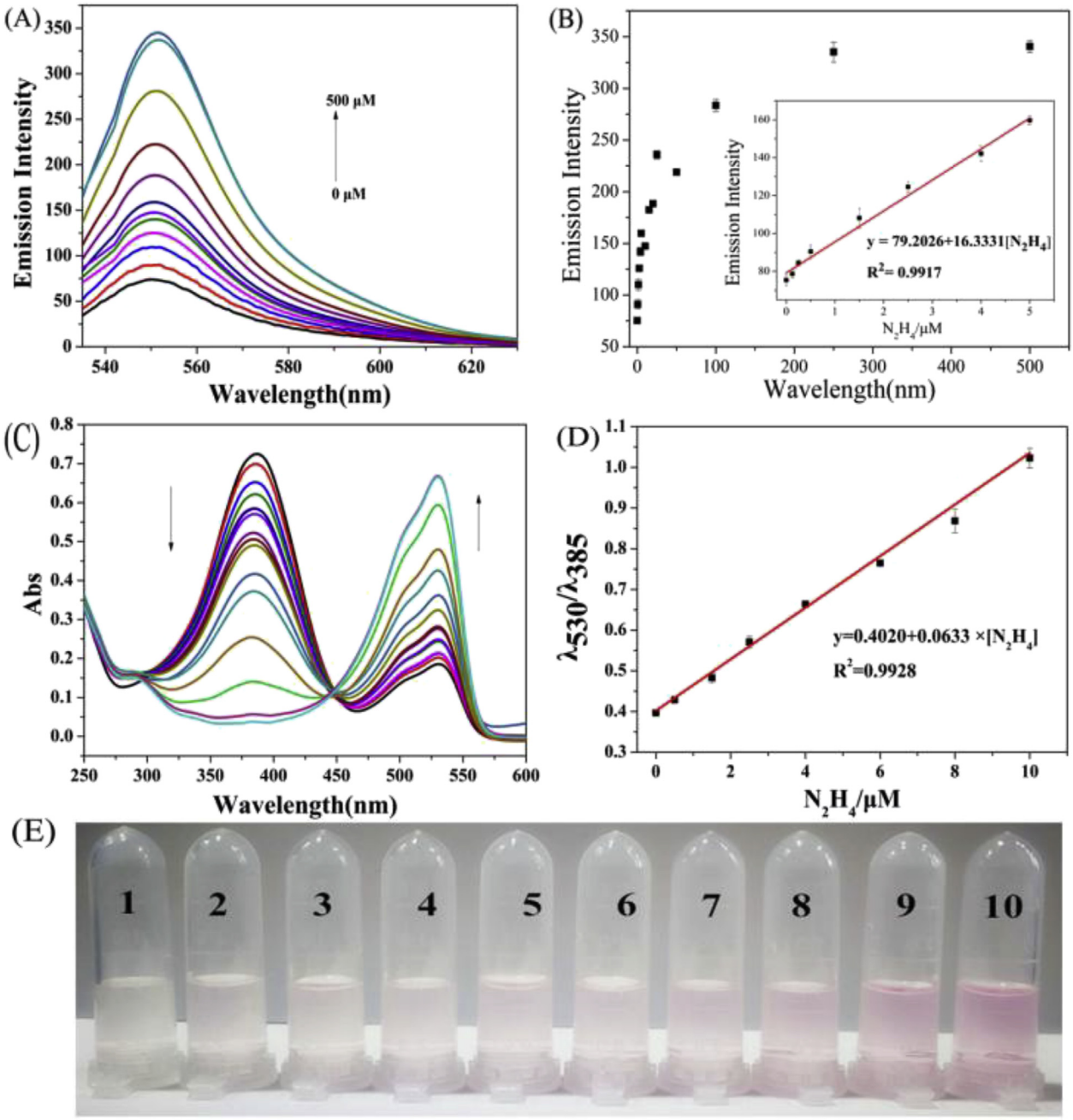

Fig. 5. (A) Fluorescence changes were recorded after addition of N_2H_4 (0.0, 0.125, 0.25, 0.5, 1.50, 2.5, 4.0, 5.0, 10.0, 15.0, 25.0, 50.0, 100.0, 250.0, 500.0 μM) to the probe (20 μM). (B) The linear relationship between fluorescence intensity and N_2H_4 concentration (excited at 520 nm). (C) UV–Vis absorption spectra were recorded after addition of N_2H_4 (0, 0.5, 1.5, 2.5, 4.0, 5.0, 10.0, 15.0, 25.0, 50.0, 100.0, 250.0, 500.0 μM) to the probe (20 μM). (D) Linear relationship between UV/Vis absorbance ratio R ($\lambda_{530}/\lambda_{385}$) and N_2H_4 concentration; (E) The color change of **McyA** upon addition of N_2H_4 (1–10: 0.0, 0.5, 1.5, 2.5, 4.0, 5.0, 10.0, 15.0, 25.0, 50.0 μM) under nature light conditions. Each picture was recorded at 20 min after the addition of N_2H_4. Conditions: DMSO/H_2O solution (1:4, v/v, 10 mM PBS, pH = 7.4).

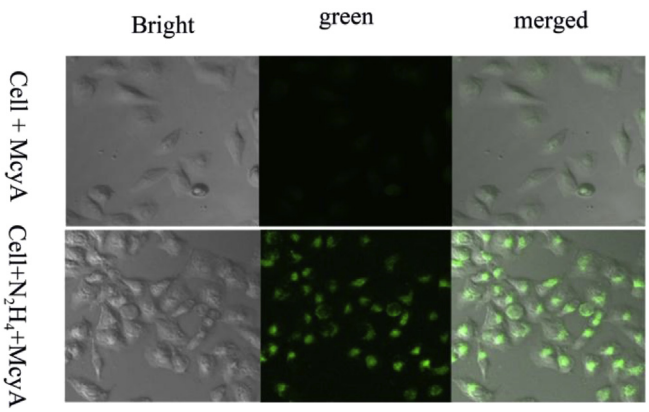

Fig. 6. Confocal fluorescence imaging of N_2H_4 in the HepG2 cells stained with 10 μM **McyA**; Control group: cells were treated with only **McyA** (10 μM) at 37 °C for 20 min (at the top). Tested group: Cells were pretreated with N_2H_4 (50 μM) and then added **McyA** (10 μM) at 37 °C for 20 min (at the bottom). Excited at 514 nm; emission was collected at 535–590 nm.

energy gap (HOMO-LUMO) of **McyOH** (2.086 eV) is significantly lower than that of **McyA** (2.305 eV), which allows us to predict the recovery of the D-π-A feature of **McyOH** and the red-shift character by N_2H_4-caused cleavage in absorption [49]. Therefore, the theory calculations are support the above anticipation, which rationalize the ICT process. Furthermore, UHPLC analysis was also employed to testify the reactive product of **McyA** and N_2H_4. As shown in Fig. S7, the retention time of the **McyA** is 1.58 min. When the different equivalents (0, 2.5, 5.0 and 12.5 equiv) of N_2H_4 were added, the intensity of the **McyA** chromatographic peak gradually reduced and the chromatographic peak of the **McyOH** (at retention time of 2.40 min) gradually increased. It agrees with the previous results (in section 3.2) and illustrates the product of **McyOH**.

3.5. Optimization of detection conditions

3.5.1. pH stability study

It is vital that the proposed probe can be operated in the wide pH range, especially in the physiological environment. Thus, the pH effect on fluorescence response of the probe **McyA** to N_2H_4 was examined at different pH values. Fig. S8A displays the low fluorescence signal of the probe in the presence of N_2H_4 in the pH range from 4.0 to 6.0. It should be attributed to the protonation of N_2H_4 at relatively low pH value, which hinders the nucleophilic attack ability of N_2H_4 for the probe [41]. Delightedly, Fig. S8A also exhibits a strong fluorescence signal of the probe treated with N_2H_4 and it is primary stable in the pH range of 7.0–10.0, which indicates that the probe **McyA** can provide a stable fluorescence response for detection of N_2H_4 under physiological conditions.

3.5.2. Response time study

The response time of the synthesized probe to N_2H_4 was examined. Fig. S8B shows that the addition of N_2H_4 (100 μM) to **McyA** (20 μM) leads to a great fluorescence enhancement at 553 nm with an increase of time until equilibrium is reached after 20 min. Therefore, 20 min was selected as the response time of the probe to N_2H_4.

3.6. The fluorescence titration experiments

Under the optimal detection conditions, the mixture solution of the **probe** (20 μM) and different concentration of N_2H_4 (0,0.125,0.25, 0.5, 1.5, 2.5, 4.0, 5.0, 10.0, 15.0, 25.0, 50.0, 100.0, 250.0, 500.0 μM) in PBS buffer (10 mM, pH = 7.4, 20% DMSO) were performed to fully assess the viability of **McyA** as a fluorescent probe. Fig. 5A displays that the fluorescence intensities of the **probe** are nearly proportional to N_2H_4 concentration range from 0.125 to 5.0 μM with a correlation coefficient ($R^2 = 0.9917$) and a standard deviation ($\sigma = 0.23$ μM) (Fig. 5B). Based on the linearity of the fluorescence titration experiment, the detection limit (LOD) for N_2H_4 is 0.042 μM (1.3 ppb, S/N = 3, at pH 7.4 in DMSO/H_2O (1:4, v/v, PBS, 10 mM), which is sufficiently lower than the threshold limit value (TLV) of N_2H_4 in drinking water (10 ppb) [13]. Meantime, a gradually increase of the peak ratio ($\lambda_{530}/\lambda_{385}$) in UV/Vis absorption spectra can be observed with the increase of N_2H_4 concentration, obtaining a good linear equation with R^2 of 0.9928 and LOD of 0.14 μM (4.5 ppb) (Fig. 5C and D). As shown in Fig. 5E, with increasing concentrations of N_2H_4, the color of mixture solution increases gradually under natural light. These results indicate that **McyA** can be utilized as fluorescent and ratiometric colorimetric dual-mode sensor for quantitative detection of N_2H_4. Finally, we compared the probe **McyA** with other probes based on an acetyl group as a recognition group (Table S1). It is found that the probe **McyA** has certain advantages in the detection limit compared with the reported work (Table S1). However, the shorter stokes shift needs to be further improved.

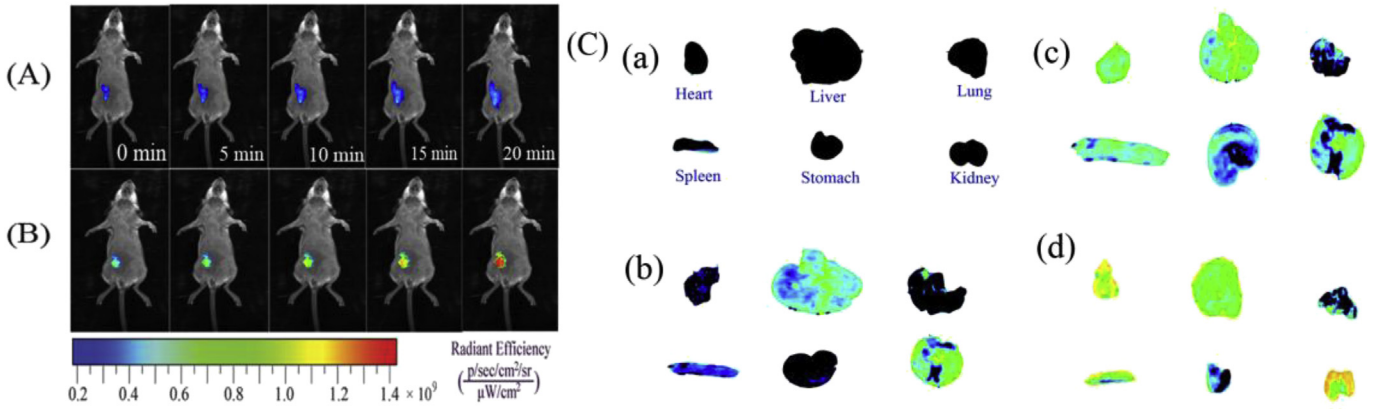

Fig. 7. (A) Representative fluorescence images (pseudocolor) of a Kunming mouse given a skin-pop injection of **McyA** (100 μL, 50 μM in a mixture of PBS buffer (pH 7.4, 10 mM, 20% DMSO). (B) Mouse given a skin-pop injection of **McyA** (100 μL, 50 μM) and given a subsequent skin-pop injection of N_2H_4 (50 μL, 500 μM). Images of (A) and (B) were taken after incubation for 0, 5, 10, 15, 20 min, respectively. (C) In vivo images of heart, liver, lung, spleen, stomach and kidney from mouse (a, the control group) feed with drinking water and from mouse (b–d) feed with drinking water containing 5 ppb (b), 10 ppb (c) and 15 ppb(d) N_2H_4, respectively. Incubated with **McyA** (50 μM) for 20 min, respectively. Excited at 514 nm; emission was collected at 535–590 nm.

3.7. Determination of N_2H_4 in real samples

In order to validate the practicality of the probe, the proposed method was applied for determining N_2H_4 in Yellow river water, tap water and diluted human serum samples. Furthermore, the recovery experiments of N_2H_4 in the spiked samples were carried out and recoveries were calculated, which shows satisfactory recoveries as well as relative standard deviation (RSD) values (Table S2), indicating that **McyA** can be used as the probe to qualify N_2H_4 in environmental and biological samples.

3.8. Bioimaging of N_2H_4 in living cells and tissues

3.8.1. Imaging of N_2H_4 in living cells

In order to further extend the application of **McyA** in biological system, the cytotoxicity experiments in living cells were performed by MTT assay using standard cell viability protocols (Fig. S9). The result shows that more than 98% cells survive in the present of 10 μM **McyA.** Even at 25 μM of **McyA**, the cell viability still remained over 80%, indicating the low cytotoxicity of McyA. Furthermore, the probe was tested for imaging of N_2H_4 in the HepG2 living cells. As illustrated in Fig. 6, the intracellular fluorescence images exhibit discernible green fluorescence in the presence of N_2H_4 compared to the control group. Subsequently, HepG2 cells that pretreated with different concentrations of N2H4 (0.0, 3.0, 5.0, 50.0, 150.0 μM) and incubated with **McyA** (10 μM) for 20 min, respectively. Fig. S10 shows a concentration-dependent change in brightness, illuminating the synthesized probe can be applied for semiquantitative assessment of N_2H_4 in living cells.

3.8.2. Mice skin-pop imaging

Encouraged by the successful cellular imaging experiments, the feasibility study for further monitoring N_2H_4 *in vivo* by the proposed probe was examined. As shown in Fig. 7A, in the control group, the mouse injected with only **McyA** (100 μL, 50 μM) for 10 min shows almost no fluorescence. However, when the mice were injected intraperitoneally with 100 μL of 50 μM **McyA** and followed injected with 50 μL of 500 μM N_2H_4, the mouse image shows increased fluorescence intensity with an increase of time (0, 5, 10, 15, 20 min, Fig. 7B). The results further confirm that the probe **McyA** can be used to visualize N_2H_4 *in vivo*.

3.8.3. Bioaccumulation tests of N_2H_4 in mice

Assay of the bioaccumulation of a toxicant in the tissues will provide information on possible health risk to both humans and other animals. Herein, the drinking water containing the different concentration of N_2H_4 (0, 5, 10, 15 ppb) was used to food mice and the bioaccumulation of N_2H_4 in organs of mice was evaluated. Fig. 7C illustrates that N_2H_4 bioaccumulation through digestion is significant in heart, liver, spleen and kidney, particularly in the liver and kidney. It is consistent with metabolic pathways. Notably, it is validated in the experiments that the presence of 5.0 ppb N_2H_4 in drinking water has been able to result in the bioaccumulation of N_2H_4 in the liver and kidney.

4. Conclusions

In summary, we have synthesized a simple Merocyanine-based dual-mode optical probe (**McyA**) for the specific detection of N_2H_4. The probe reveals a remarkable fluorescent enhancement at 553 nm in the presence of N_2H_4 with high selectivity toward common interfering ions and compounds. Simultaneously, it also presents a ratiometric colorimetric sensor property for naked eye detection of N_2H_4 in real samples. Moreover, the imaging application of the probe in vitro and *in vivo* was achieved with good cell-membrane permeability and low cytotoxicity, disclosing that the established approach can be utilized as an efficient means for convenient detecting, tracking hydrazine in environmental and biological sample.

Acknowledgement

This work was supported by the National Natural Science Foundation of China (NSFC) Fund (No.21575055), the Fundamental Research Funds for the Central Universities (lzujbky-2017-k09) and Henan Key Laboratory of Biomolecular Recognition and Sensing (HKLBRSK1802).

Appendix A. Supplementary data

Supplementary data to this article can be found online at https://doi.org/10.1016/j.saa.2019.117625.

References

[1] R. Seshadri, M. Israel, W.J. Pegg, Adriamycin analogues. Preparation and biological evaluation of some novel 14-thiaadriamycins, J. Med. Chem. 14 (1983) 11–15.
[2] I.C. Vieira, K.O. Lupetti, O. Fatibello-Filho, Sweet potato (ipomoea batatas (L.) LAM.) tissue as biocatalyst in a paraffin/graphite biosensor for hydrazine in boiler feed water, Anal. Lett. 35 (2002) 2221–2231.
[3] K. Yamada, K. Yasuda, N. Fujiwara, Z. Siroma, H. Tanaka, Y. Miyazaki, T. Kobayashi, Potential application of anion-exchange membrane for hydrazine fuel cell electrolyte, Electrochem. Commun. 5 (2003) 892–896.
[4] S. Garrod, M.E. Bollard, A.W. Nicholls, S.C. Connor, J. Connelly, J.K. Nicholson, E. Holmes, Integrated metabonomic analysis of the multiorgan effects of hydrazine toxicity in the rat, Chem. Res. Toxicol. 18 (2005) 115–122.
[5] G. Yue, Q. Zeng, J. Huang, L. Wang, Mechanism studies of hydrazine electrooxidation by a platinum ultramicroelectrode: effects of supporting electrolytes, J. Electroanal. Chem. (2018) 19–25.
[6] W.X. Yin, Z.P. Li, J.K. Zhu, H.Y. Qin, Effects of NaOH addition on performance of the direct hydrazine fuel cell, J. Power Sources 182 (2008) 520–523.
[7] U. Ragnarsson, Synthetic methodology for alkyl substituted hydrazines, Chem. Soc. Rev. 30 (2001) 205–213.
[8] A. Serov, K. Chan, Direct hydrazine fuel cells: a review, Appl. Catal. B Environ. 98 (2010) 1–9.
[9] J.E. Troyan, Properties, production, and uses of hydrazine, Ind. Eng. Chem. 45 (1953) 2608–2612.
[10] P.M. Terlizzi, H. Strem, Correction - liquid propellant handling, transfer, and storage, Ind. Eng. Chem. 48 (1956) E787.
[11] N. Listed, Re-evaluation of some organic chemicals, hydrazine and hydrogen peroxide. Proceedings of the IARC Working Group on the Evaluation of Carcinogenic Risks to Humans. Lyon, France, IARC Monogr. Eval. Carcinog. Risks Hum. 71 (Pt 1) (1999) 1, 17-24 February 1998.
[12] A. Umar, M.M. Rahman, S.H. Kim, Y.B. Hahn, Zinc oxide nanonail based chemical sensor for hydrazine detection, Chem. Commun. 2 (2007) 166–168.
[13] H.L. Min, B. Yoon, J.S. Kim, J.L. Sessler, Naphthalimide trifluoroacetyl acetonate: a hydrazine-selective chemodosimetric sensor, Chem. Sci. 4 (2013) 4121–4126.
[14] Y.Y. Liu, I. Schmeltz, D. Hoffmann, Chemical studies on tobacco smoke. Quantitative analysis of hydrazine in tobacco and cigarette smoke, Anal. Chem. 46 (1974) 885–889.
[15] D.P. Elder, D. Snodin, A. Teasdale, Control and analysis of hydrazine, hydrazides and hydrazones–genotoxic impurities in active pharmaceutical ingredients (APIs) and drug products, J. Pharm. Biomed. 54 (2011) 900–910.
[16] M. Sun, L. Bai, D.Q. Liu, A generic approach for the determination of trace hydrazine in drug substances using in situ derivatization-headspace GC-MS, J. Pharm. Biomed. 49 (2009) 529–533.
[17] H. Bhutani, S. Singh, S. Vir, K.K. Bhutani, R. Kumar, A.K. Chakraborti, K.C. Jindal, LC and LC-MS study of stress decomposition behaviour of isoniazid and establishment of validated stability-indicating assay method, J. Pharm. Biomed. 43 (2007) 1213–1220.
[18] C. Batchelor-Mcauley, C.E. Banks, A.O. Simm, T.G. Jones, R.G. Compton, The electroanalytical detection of hydrazine: a comparison of the use of palladium nanoparticles supported on boron-doped diamond and palladium plated BDD microdisc array, Analyst 131 (2005) 106–110.
[19] H.E. Malone, Determination of mixtures of hydrazine and 1,1-dimethylhydrazine, Anal. Chem. 48 (2002) 575–577.
[20] J. Ma, J. Fan, H. Li, Q. Yao, J. Xia, J. Wang, X. Peng, Probing hydrazine with a near-infrared fluorescent chemodosimeter, Dyes Pigments 138 (2017) 39–46.
[21] C. Hu, W. Sun, J. Cao, P. Gao, J. Wang, J. Fan, F. Song, S. Sun, X. Peng, A ratiometric near-infrared fluorescent probe for hydrazine and its in vivo applications, Org. Lett. 15 (2013) 4022–4025.
[22] Y. Hao, Y. Zhang, K. Ruan, F. Meng, T. Li, J. Guan, L. Du, P. Qu, M. Xu, A highly selective long-wavelength fluorescent probe for hydrazine and its application in living cell imaging, Spectrochim. Acta 184 (2017) 355–360.

[23] W. Li, C.X. Yang, X.P. Yan, A versatile covalent organic framework-based platform for sensing biomolecules, Chem. Commun. 53 (2017) 11469–11471.
[24] H.L. Qian, C. Dai, C.X. Yang, X.P. Yan, High crystallinity covalent organic framework with dual fluorescence emissions and its ratiometric sensing application, ACS Appl. Mater. Interfaces 9 (2017) 24999–25005.
[25] Y. Xu, X.H. Jia, X.B. Yin, X.W. He, Y.K. Zhang, Carbon quantum dot stabilized gadolinium nanoprobe prepared via a one-pot hydrothermal approach for magnetic resonance and fluorescence dual-modality bioimaging, Anal. Chem. 86 (2014) 12122–12129.
[26] X.F. Yang, Q. Huang, Y. Zhong, Z. Li, H. Li, M. Lowry, J.O. Escobedo, R.M. Strongin, A dual emission fluorescent probe enables simultaneous detection of glutathione and cysteine/homocysteine, Chem. Sci. 5 (2014) 2177–2183.
[27] X. Yang, Y. Guo, R.M. Strongin, A seminaphthofluorescein-based fluorescent chemodosimeter for the highly selective detection of cysteine, Org. Biomol. Chem. 10 (2012) 2739–2741.
[28] H. Tse, Q. Li, S. Chan, Q. You, A.W.M. Lee, W. Chan, A ratiometric fluorescent and colorimetric probe for selective detection of hydrazine, RSC Adv. 6 (2016) 14678–14681.
[29] J. Zhang, L. Ning, J. Liu, J. Wang, B. Yu, X. Liu, X. Yao, Z. Zhang, H. Zhang, Naked-eye and near-infrared fluorescence probe for hydrazine and its applications in in vitro and in vivo bioimaging, Anal. Chem. 87 (2015) 9101–9107.
[30] Y.Z. Ran, H.R. Xu, K. Li, K.K. Yu, J. Yang, X.Q. Yu, Development of a mitochondria-targeted fluorescent probe for hydrazine monitoring in living cells, RSC Adv. 6 (2016) 14678–14681.
[31] A.K. Mahapatra, P. Karmakar, S. Manna, K. Maiti, D. Mandal, Benzthiazole-derived chromogenic, fluorogenic and ratiometric probes for detection of hydrazine in environmental samples and living cells, J. Photochem. Photobiol., A 334 (2017) 1–12.
[32] X. Xia, F. Zeng, P. Zhang, J. Lyu, Y. Huang, S. Wu, An ICT-based ratiometric fluorescent probe for hydrazine detection and its application in living cells and in vivo, Sens. Actuators B Chem. 227 (2016) 411–418.
[33] G. Yu, Y. Cao, H. Liu, Q. Wu, Q. Hu, B. Jiang, Z. Yuan, A spirobenzopyran-based multifunctional chemosensor for the chromogenic sensing of Cu^{2+} and fluorescent sensing of hydrazine with practical applications, Sensor Actuator B Chem. 245 (2017) 803–814.
[34] S. Chen, P. Hou, J. Wang, L. Liu, Q. Zhang, A highly selective fluorescent probe based on coumarin for the imaging of N2H4 in living cells, Spectrochim. Acta 173 (2017) 170–174.
[35] Q. Yong, L. Jie, L. Han, L. Lin, H. Zhu, A resorufin-based colorimetric and fluorescent probe for live-cell monitoring of hydrazine, Biosens. Bioelectron. 58 (2014) 282–286.
[36] S. Goswami, K. Aich, S. Das, S.B. Roy, B. Pakhira, S. Sarkar, A reaction based colorimetric as well as fluorescence 'turn on' probe for the rapid detection of hydrazine, RSC Adv. 4 (2014) 14210–14214.
[37] S. Zhu, W. Lin, L. Yuan, Development of a near-infrared fluorescent probe for monitoring hydrazine in serum and living cells, Anal Methods 5 (2013) 3450–3453.
[38] S. Yu, S. Wang, H. Yu, Y. Feng, S. Zhang, M. Zhu, H. Yin, X. Meng, A ratiometric two-photon fluorescent probe for hydrazine and its applications, Sensor Actuator B Chem. 220 (2015) 1338–1345.
[39] M.G. Choi, J. Hwang, J.O. Moon, J. Sung, S.K. Chang, Hydrazine-Selective chromogenic and fluorogenic probe based on levulinated coumarin, Org. Lett. 13 (2011) 5260–5263.
[40] S. Nandi, A. Sahana, S. Mandal, A. Sengupta, A. Chatterjee, D.A. Safin, M.G. Babashkina, N.A. Tumanov, Y. Filinchuk, D. Das, Hydrazine selective dual signaling chemodosimetric probe in physiological conditions and its application in live cells, Anal. Chim. Acta 893 (2015) 84–90.
[41] W. Chen, W. Liu, X.J. Liu, Y.Q. Kuang, R.Q. Yu, J.H. Jiang, A novel fluorescent probe for sensitive detection and imaging of hydrazine in living cells, Talanta 162 (2017) 225–231.
[42] T.D. Kim, K.S. Lee, D-π-A conjugated molecules for optoelectronic applications, Macromol. Rapid Commun. 36 (2015) 943–958.
[43] d.S. AP, G. HQ, G. T, H. AJ, M. CP, R. JT, R. TE, Signaling recognition events with fluorescent sensors and switches, Chem. Rev. 97 (1997) 1515–1566.
[44] S.P. Wang, W.J. Deng, D. Sun, M. Yan, H. Zheng, J.G. Xu, A colorimetric and fluorescent merocyanine-based probe for biological thiols, Org. Biomol. Chem. 7 (2009) 4017–4020.
[45] J. Fan, W. Sun, M. Hu, J. Cao, G. Cheng, H. Dong, K. Song, Y. Liu, S. Sun, X. Peng, An ICT-based ratiometric probe for hydrazine and its application in live cells, Chem. Commun. 48 (2012) 8117–8119.
[46] Y. Tan, J. Yu, J. Gao, Y. Cui, Y. Yang, G. Qian, A new fluorescent and colorimetric probe for trace hydrazine with a wide detection range in aqueous solution, Dyes Pigments 99 (2013) 966–971.
[47] G. Qian, Z., Y. Wang, Near-Infrared organic compounds and emerging applications, Chem. Asian J. 5 (2010) 1006–1029.
[48] N. Kartonlifshin, E. Segal, L. Omer, M. Portnoy, R. Satchifainaro, D. Shabat, A unique paradigm for a Turn-ON near-infrared cyanine-based probe: noninvasive intravital optical imaging of hydrogen peroxide, J. Am. Chem. Soc. 133 (2011) 10960–10965.
[49] L. Fan, W. Zhang, X. Wang, W. Dong, Y. Tong, C. Dong, S. Shuang, A two-photon ratiometric fluorescent probe for highly selective sensing of mitochondrial cysteine in live cells, Analyst 144 (2019) 439–447.